EUROPEAN COOPERATION
IN THE FIELD OF SCIENTIFIC
AND TECHNICAL RESEARCH

EURO-COST

COST 2100 TD(08) 436
Wroclaw, Poland
February 6–8, 2008

SOURCE:
[1]Institut für Nachrichten- und Hochfrequenztechnik, Technische Universität Wien, Vienna, Austria
[2]Forschungszentrum Telekommunikation Wien (ftw.), Vienna, Austria
[3]Department of Electrical and Information Technology, Lund University, Lund, Sweden
[4]Mitsubishi Electric Research Labs, Cambridge, USA

Comparison of Lund'07 vehicular channel measurements with the IEEE 802.11p channel model

Alexander Paier[1], Johan Karedal[3], Nicolai Czink[1,2],
Charlotte Dumard[2], Thomas Zemen[2], Fredrik Tufvesson[3],
Christoph F. Mecklenbräuker[1], Andreas F. Molisch[3,4]

[1]Institut für Nachrichten- und Hochfrequenztechnik
Gusshausstrasse 25/389
1040 Vienna
AUSTRIA
Phone: +43 1 58801 38951
Fax: +43 1 58801 38999
Email: apaier@nt.tuwien.ac.at

Comparison of Lund'07 vehicular channel measurements with the IEEE 802.11p channel model

Alexander Paier[1], Johan Karedal[2], Nicolai Czink[1,3], Charlotte Dumard[3],
Thomas Zemen[3], Fredrik Tufvesson[2], Andreas F. Molisch[2,4], Christoph F. Mecklenbräuker[1]

[1]Institut für Nachrichtentechnik und Hochfrequenztechnik, Technische Universität Wien, Vienna, Austria
[2]Department of Electrical and Information Technology, Lund University, Lund, Sweden
[3]Forschungszentrum Telekommunikation Wien (ftw.), Vienna, Austria
[4]Mitsubishi Electric Research Labs, Cambridge, USA
Contact: apaier@nt.tuwien.ac.at

***Abstract*— This paper presents a very preliminary comparison between the IEEE 802.11p channel model parameters with parameters evaluated from new high speed measurements in Lund, Sweden. Following interesting differences as well as similarities are observed: The measured maximum excess delay is about one fifth of the one proposed in the IEEE 802.11p model. The amplitude distribution for each tap can be approximated as Ricean distribution, with a very high Rice factor for the first tap and small Rice factors for later taps. Similar to the IEEE 802.11p model we observe a strong line of sight path near to the Doppler frequency of zero and weaker paths at Doppler frequencies about twice the measurement vehicle's speed. As a key result we show that the average delay-Doppler spectra, which is one part of the tap delay model, does *not* reflect the time variant behavior of the radio channel.**

I. Introduction

Few vehicular radio channels in the 5 GHz band have been measured with sufficient resolution in the delay- and Doppler-domains to characterize the time-selective fading of future vehicular broadband links. Such measurements are needed to validate the reliability and throughput of traffic telematics services delivered via IEEE 802.11p [1]. There exist only a few single-antenna measurements at 2.4 GHz, e.g. [2], [3], and in [4] narrow-band measurements at 5.2 GHz are investigated. Also the channel model standardized by IEEE 802.11p [1] was based on [2] and [3]. While this model and the measurements it is based on have been carefully conducted and have proven highly valuable for the development of the 11p standard, the question still remains whether measurements in other environments would give different results.

For this reason, we carried out high speed vehicular broadband 4×4 MIMO channel measurements in the frequency band 5.08-5.32 GHz in Lund, Sweden, in April 2007. The choice of the measurement band was dictated by regulatory concerns, as well as the availability of calibrated antenna arrays. This band is rather close to the 5.9 GHz band and we do not expect any significant differences in channel statistics. Results from this measurement campaign for different environments are presented in [5] and [6]. In this paper we compare the significant parameters of the 11p standard model with the parameters extracted from our vehicle-to-vehicle (V2V) measurements. The methods used in this paper are preliminary, more advanced tests need to be undertaken.

II. Measurements

A. Measurement Equipment

Our measurement campaign was carried out with the RUSK Lund channel sounder which is based on the "switched-array" principle [7]. In Tab. I the main measurement parameters are listed. A detailed description of the measurement equipment and setup can be found in [5].

B. Measurement Scenario

We consider a highway V2V scenario in order to allow further comparison to the proposed model in the draft standard IEEE 802.11p [1], because this model is also based on V2V highway measurements. Fig. 1

TABLE I

MEASUREMENT PARAMETERS

Center frequency, f	5.2 GHz
Measurement bandwidth, BW	240 MHz
Delay resolution, $\Delta\tau = 1/BW$	4.17 ns
Transmit power, P_{Tx}	27 dBm
Test signal length, τ_{max}	3.2 μs
Number of Tx antenna elements, N_{Tx}	4
Number of Rx antenna elements, N_{Rx}	4
Snapshot time, t_{snap}	102.4 μs
Snapshot repetition rate, t_{rep}	307.2 μs
Number of snapshots, N	32500
Recording time, t_{rec}	10 s
File size, FS	1 GB
Tx antenna height, h_{Tx}	2.4 m
Rx antenna height, h_{Rx}	2.4 m

shows a satellite photograph (source [8]) of the investigated highway and in Fig. 2 a photograph taken during the measurements of the highway scenario is presented. Both vehicles were driving in the same direction. 19 measurements, each with a length of 10 s, were carried out in this scenario. In the following we will call such a single measurement with 10 s duration a *measurement run*. The speed of the measurement vehicles was 25 m/s (90 km/h) in 10 measurement runs and 29 m/s (105 km/h) in the other 9 measurement runs. Also the distance between the two vehicles was varied between 50 m and 150 m, where we tried to keep the distance constant during each measurement run.

Fig. 1. Satellite photo of the highway (source: [8])

III. EVALUATION RESULTS

From our measurements we evaluated the significant parameters of the IEEE 802.11p channel model

Fig. 2. Photo of the highway in the east of Lund

in order to compare them accordingly. The 11p channel model is a tap delay model, with 10 taps. For each tap, the power, the excess delay, the Rice factor, and significant parameters describing the Doppler spectrum, are given. A detailed description of the derivation of the IEEE 802.11p model can be found in [3]. In the following section, Sec. III-A, we describe the evaluation of the parameters from our measurements: Tap power and tap Rice factor. In Sec. III-B we analyze the extracted parameters and compare them with the 11p model parameters. Sec. III-C describes the disadvantages of the 11p model by means of the delay-Doppler spectrum.

A. Parameter Evaluation

We calculated the average power-delay profiles (PDPs) by averaging over $L = 232$ snapshots in the time domain and taking the sum over all $P = 16$ channels of the measured 4×4 MIMO channel

$$P_{\text{PDP}}(k\Delta\tau) = \frac{1}{L}\sum_{n=0}^{L-1}\sum_{p=1}^{P}|h(nt_{\text{rep}}, k\Delta\tau, p)|^2.$$

An averaging over 232 snapshots is equal to 71 ms and approximately 30 wavelengths at 25 m/s. We assume a wide-sense stationary radio channel over this duration. In order to limit the noise contribution we set all values smaller than the noise threshold of 6 dB above the noise level to zero. Further we selected only these average PDPs that showed a peak-to-noise ratio greater than 35 dB. Each average PDP was normalized to its maximum. Fig. 3 shows the normalized average PDPs of our measurements. The maximum of each segment corresponds to the line of sight (LOS) path and was shifted to delay bin zero. After a delay of 200 ns we observe only a few significant parts of this average PDPs. This is much less than the delay duration of approximately 1 μs found in [3].

In order to make a comparison with the 11p model we use the same number of taps, $M = 10$, as in [3]. In

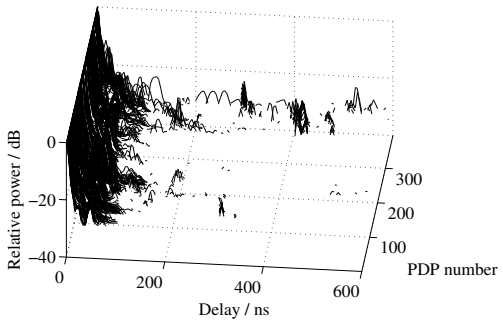

Fig. 3. Average PDPs

[3] the length of each tap is equal to the delay resolution of 50 ns. So the tap delay has equidistant values 0 ns, 50 ns, 100 ns, etc. The delay resolution of our measurements, $\Delta\tau = 4.17$ ns, is much higher. In order to get the same tap delay we have to use $I = 12$ delay bins for each tap.

The power for each tap can be obtained by

$$P_m(\tau_m) = \frac{1}{I} \sum_{k=i_m}^{i_m+I-1} P_{\text{PDP}}(k\Delta\tau),$$

for $0 \leq m \leq M-1$, where M is the number of taps and i_m is the delay bin number at the start of each tap.

By investigating the amplitude distribution of the taps we found that a Ricean distribution, [9], fits very well, see Sec. III-B. As in the 11p channel model we evaluated the Rice factor, describing this amplitude distribution. We calculated the Rice factor, K_{Rice}, using the moment-method, described in [10]. With this calculation we obtain a Rice factor, K_{Rice}, for each delay bin of the individual PDPs. In order to get the mean Rice factor for each tap we were averaging K_{Rice} over the $I = 12$ delay bins associated with each tap.

B. Parameter Comparison

Tab. II presents the estimated 10-tap model parameters from our V2V highway scenario measurements. Column one presents the tap number, column two the tap delay, the third column the relative tap power in dB, and column four shows the tap Rice factor.

The relative tap power in Tab. II is the mean over the tap power of all average PDPs. The tap power of the second tap is 20.2 dB below the power of the first tap. All other tap powers are more than 29 dB lower than the maximum in the first tap. Considering the minimum peak-to-noise ratio of the average PDPs of 35 dB, see Sec. III-A, and the noise threshold of 6 dB above the noise level, we can discard all powers

TABLE II
ESTIMATED TAP MODEL PARAMETERS

Tap	Tap delay ns	Tap power dB	K_{Rice}
1	0	0.0	193.96
2	50	−20.2	10.34
3	100	−29.9	1.63
4	150	−33.4	0.66
5	200	−36.2	0.30
6	250	−37.1	0.24
7	300	−33.5	0.23
8	350	−40.5	0.13
9	400	−32.9	0.08
10	450	−38.7	0.05

lower than 29 dB below the first tap. Compared with the 11p model, the tap power extracted from our measurements decreases much faster, e.g. the tap power of tap 2 of the 11p model is equal to −6.5 dB. A possible explanation for this is the different highway environment in our measurement campaign. Considering also the tap powers below −29 dB we observe some later taps with higher power, e.g. tap 9 with −32.9 dB. In Fig. 3 we find that this power is coming only from a few average PDPs, at a delay of approximately 400 ns. This shows the temporal variation of the V2V radio channel, which is not reflected by the 10-tap delay 11p model. We will focus on this time variance in more detail in the delay-Doppler spectra in Sec. III-C.

An investigation of the amplitude distribution of the taps yielded a Ricean distribution. The ratio of the power in the LOS component to the power in the diffuse component is called the Rice factor K_{Rice}. Fig. 4 presents a typical amplitude distribution over approximately 30 wavelengths for the first tap compared with a Ricean distribution. We see that this Ricean shape fits very well to our amplitude distribution. In Fig. 5 typical amplitude distributions for tap 2 and tap 5 are presented, where we also observe a Ricean behavior.

Tab. II presents the estimated *median* Rice factor of our measurements. We observe a high Rice factor for tap 1, which is congruent with a strong LOS path in this tap. Also the value of 10.3 for the Rice factor of tap 2 represents a tap with a dominant component. From tap 4 to 10 the Rice factors are smaller than one, which can be interpreted by a more or less equally distributed power of all arriving paths. The estimated Rice factors are in the same range as in the 11p model. In Fig. 6 the cumulative distribution function (CDF) is shown. We can see that there are also considerably

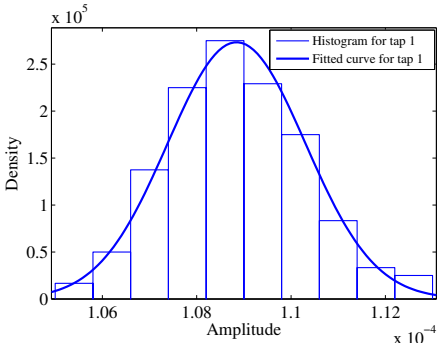

Fig. 4. Amplitude statistics for tap 1

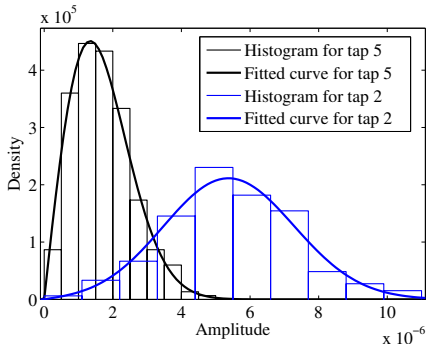

Fig. 5. Amplitude statistics for tap 2 and tap 5

high Rice factors in the first tap. Approximately 10 % of the Rice factors are greater than 700.

C. Doppler Spectrum Comparison

We calculated the delay-Doppler spectrum using the Fourier transformation over a time duration of 71 ms (232 snapshots) and taking the sum of the magnitude squared of the terms over all 16 channels of the measured 4×4 MIMO channel

$$P_{\mathrm{DD}}(r\Delta\nu, k\Delta\tau) = \sum_{p=1}^{P} |f_{\mathrm{fft}}(h(nt_{\mathrm{rep}}, k\Delta\tau, p))|^2.$$

The duration of 71 ms was taken because the wide-sense stationary and uncorrelated scatterer (WSSUS)

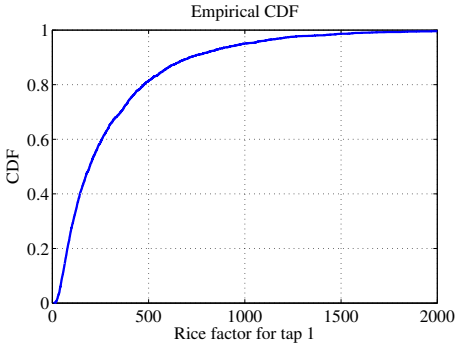

Fig. 6. CDF of the Rice factor for tap 1

condition is approximately fulfilled within that window. With our measurement setup and this Fourier transformation interval we achieve a Doppler resolution of 14 Hz and a maximum resolvable Doppler frequency of 1.6 kHz.

Fig. 7 shows an example of one delay-Doppler spectrum from a measurement with a speed of 25 m/s. We observe a strong LOS path near a Doppler frequency of zero, which fits to the driving scenario where both vehicles are traveling in the same direction with approximately the same speed. Important are the two peaks at a delay of approximately 500 ns and a Doppler shift of approximately ± 850 Hz. Peaks with this Doppler shifts were also found in all other delay-Doppler spectra at variant delays. A Doppler frequency of 850 Hz corresponds to a speed of 49 m/s, at our center frequency of 5.2 GHz, which is about twice the speed of our measurement vehicles. Paths with this Doppler frequency result from a single bounced stationary scatterer in driving direction, above or next to the road. Such scatterers can be overpasses or traffic signs, especially the latter ones have good reflection properties, because usually they are made of metal. The sign of this Doppler frequency depends on the relative position of the scatterer — in front or behind the measurement vehicles. Further two important peaks are observed at delays of approximately 150 ns and 300 ns and a Doppler shift of approximately 1370 Hz. These peaks are important, because in the 11p model no Doppler shifts greater than two times the vehicle's speed are modeled. In our measurements we found peaks with such a high Doppler shift, which should be included in a V2V channel model.

In order to make further comparisons with the IEEE 802.11p model we calculated an average delay-Doppler spectrum over one measurement run, as it is proposed in the standard. We would like to point out that such an averaged spectrum can not anymore be interpreted as a delay-Doppler spectrum, because the WSSUS assumption is not fulfilled over this duration. We show also that such an averaged spectrum does not reflect the time variance of a V2V radio channel that is an important characteristic of such a channel.

Fig. 8 presents the average delay-Doppler spectrum over one measurement run. As described above the two peaks in Fig. 7 at the Doppler frequencies of ± 850 Hz are moving from larger delays to smaller delays over time. We are not able do observe these single scatterers in the average delay-Doppler spectrum, because the peaks are blurred over the delay

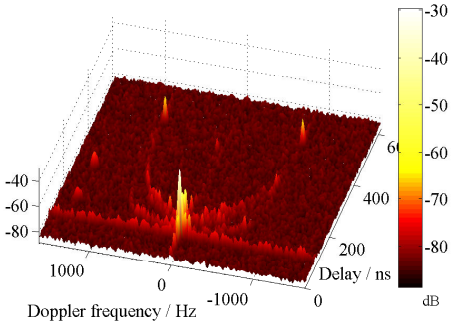

Fig. 7. Delay-Doppler spectrum of a measurement with a speed of 25 m/s

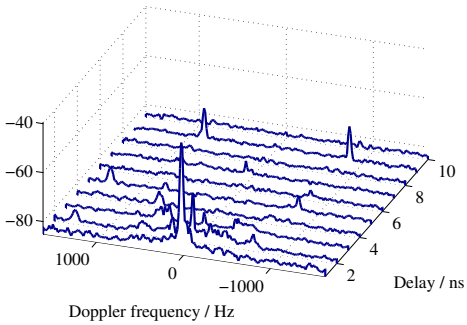

Fig. 9. Tap delay-Doppler spectrum of a measurement with a speed of 25 m/s

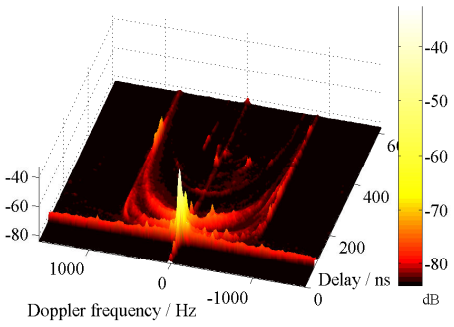

Fig. 8. Average delay-Doppler spectrum over one measurement run with a speed of 25 m/s

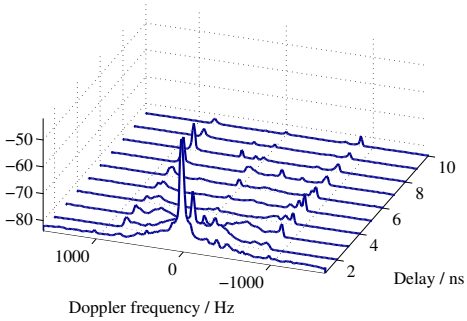

Fig. 10. Average tap delay-Doppler spectrum over one measurement run with a speed of 25 m/s

domain. Also the two peaks at the high Doppler frequency of 1370 Hz can not be found in the average delay-Doppler spectrum.

These differences between the short-time delay Doppler spectrum and the averaged spectrum are more prominent in the tap delay-Doppler spectra that are used in the 11p model. Each tap in the 11p model is described by one average delay-Doppler spectrum. For the calculation of the delay-Doppler spectra for each tap we took the mean of the delay-Doppler spectra over the 12 delay bins associated to each delay tap.

In Fig. 9 and 10 the short-time delay-Doppler spectra and the average tap delay-Doppler spectra over one measurement run are presented, respectively. The LOS peak near the Doppler frequency of zero is also present in the 11p model. By investigating the same four peaks as in the continuous delay-Doppler spectra we find some important differences. The two peaks in tap 9 in the short-time spectrum, Fig. 9, can not be found with the same power in the average spectrum, Fig. 10, but there is one peak with approximately the same power in tap 8. The other two peaks in tap 2 and tap 5 at a Doppler frequency of 1370 Hz are not anymore present in the average delay-Doppler spectra.

We conclude that the 10-tap delay model from the IEEE 802.11p standard unfortunately does not reflect the time variance behavior of the radio channel. However, this would be most important in V2V scenarios. Consiquently we developed a geometry-based stochastic MIMO V2V model considering this time variance [11].

IV. Conclusions

We observed shorter impulse responses for the Lund'07 vehicle-to-vehicle measurements than proposed by the IEEE 802.11p model. The measured maximum significant delay is about one fifth of the maximum delay of the IEEE 802.11p model. This results also in a faster decrease of the tap power. As in the 11p model we found that a Ricean distribution is the best approximation for the amplitude distribution for all taps. A large Rice factor for the first tap indicates the existence of a strong line of sight (LOS) path in this tap. Later taps (tap 4 to tap 10) showed a Rice factor less than 1. The results presented in this paper indicate that the 11p model does not reflect the time variant behavior of the channel. More thorough investigation is required to substantiate the criticism imposed.

V. Acknowledgements

We would like to thank RIEGL Laser Measurement Systems GmbH and MEDAV GmbH for their generous support. This work was carried out with partial funding from Kplus and WWTF in the ftw. projects I0 and I2 and partially by an INGVAR grant of the Swedish Strategic Research Foundation (SSF), and the SSF Center of Excellence for High-Speed Wireless Communications (HSWC), and COST 2100. Finally, we would like to thank Helmut Hofstetter for guidance and help during the measurement campaign.

References

[1] 802.11p, "Draft amendment to wireless LAN medium access control (MAC) and physical layer (PHY) specifications: Wireless access in vehicular environments," IEEE P802.11p/D0.26, January 2006.

[2] Guillermo Acosta, Kathleen Tokuda, and Mary Ann Ingram, "Measured joint doppler-delay power profiles for vehicle-to-vehicle communications at 2.4 GHz," in *Global Telecommunications Conference 2004*, 29 November – 3 December 2004.

[3] Guillermo Acosta-Marum and Mary Ann Ingram, "A BER-based partitioned model for a 2.4 GHz vehicle-to-vehicle expressway channel," *Wireless Personal Communications (WPC)*, pp. 421–443, July 2006.

[4] J. Maurer, T. Fügen, and W. Wiesbeck, "Narrow-band measurement and analysis of the inter-vehicle transmission channel at 5.2 GHz," in *Vehicular Technology Conference (VTC) 2002*, 6–9 May 2002.

[5] Alexander Paier, Johan Karedal, Nicolai Czink, Helmut Hofstetter, Charlotte Dumard, Thomas Zemen, Fredrik Tufvesson, Christoph F. Mecklenbräuker, and Andreas F. Molisch, "First results from car-to-car and car-to-infrastructure radio channel measurements at 5.2 GHz," in *International Symposium on Personal, Indoor and Mobile Radio Communications (PIMRC) 2007*, September 2007, pp. 1–5.

[6] Alexander Paier, Johan Karedal, Nicolai Czink, Helmut Hofstetter, Charlotte Dumard, Thomas Zemen, Fredrik Tufvesson, Andreas F. Molisch, and Christoph F. Mecklenbräuker, "Car-to-car radio channel measurements at 5 GHz: Pathloss, power-delay profile, and delay-Doppler spectrum," in *IEEE International Symposium on Wireless Communication Systems (ISWCS)*, October 2007, pp. 224–228.

[7] Rainer Thomä, D Hampicke, Andreas Richter, G Sommerkorn, A Schneider, U Trautwein, and Walther Wirnitzer, "Identification of time-variant directional mobile radio channels," *IEEE Trans. on Instrumentation and Measurement*, vol. 49, pp. 357–364, 2000.

[8] http://hitta.se, ," January, 2008.

[9] S. O. Rice, "Mathematical analysis of random noise," *Bell System Technical Journal*, vol. 24, pp. 46–156, January 1945.

[10] L. J. Greenstein, D. G. Michelson, and V. Erceg, "Moment-method estimation of the Ricean K-factor," *IEEE Communications Letters*, vol. 3, pp. 175–176, June 1999.

[11] Johan Karedal, Alexander Paier, Nicolai Czink, Charlotte Dumard, Thomas Zemen, Fredrik Tufvesson, Christoph F. Mecklenbräuker, and Andreas F. Molisch, "A geometry-based stochachtic MIMO model for vehicle-to-vehicle communications," *will be published in IEEE Transactions on Wireless Communications*.